1

2   PROF. DONGHYUN   KIM (Orcid ID : 0000-0002-5137-2213)

3   PROF. JONG-HWAN   PARK (Orcid ID : 0000-0003-4664-5640)

4   PROF. SANG-UK   SEO (Orcid ID : 0000-0002-6633-1932)

5

6

7   Article type   : Original Article

8

9

10   Recognition of the microbiota by Nod2 contributes to the oral adjuvant

11   activity of cholera toxin through the induction of IL-1β

12

13   Donghyun Kim,[1,2,3,4] Yu-Mi Kim,[5] Wan-Uk Kim,[5,6] Jong-Hwan Park,[7] Gabriel Núñez,[1,2,]*

14   and Sang-Uk Seo[4,8,]*

15

16   [1]*Department of Pathology, University of Michigan Medical School, Ann Arbor, MI,*

17   [2]*Comprehensive Cancer Center, University of Michigan Medical School, Ann Arbor, MI*

18   *USA,* [3]*Department of Microbiology and Immunology, Seoul National University College of*

19   *Medicine, Seoul,* [4]*Department of Biomedical Sciences, Seoul National University College of*

20   *Medicine, Seoul, [5]Center for Integrative Rheumatoid Transcriptomics and Dynamics, the*

21   *Catholic University of Korea, Seoul, [6]Department of Intestinal Medicine, College of*

22   *Medicine, the Catholic University of Korea, Seoul, [7]Laboratory Animal Medicine, College*

23   *of Veterinary Medicine and BK 21 PLUS Project Team, Chonnam National University,*

24   *Gwangju, and [8]Wide River Institute of Immunology, Hongcheon, Gangwon-do, South*

25   *Korea*

26

27   *Correspondence: Dr. Sang-Uk Seo, Wide River Institute of Immunology, Seoul National

28   University College of Medicine, 101 Dabyeonbat-gil, Hwachon-myeon, Hongcheon-gun,

29   Gangwon-do 25159, South Korea.

30   E-mail address: suseo@snu.ac.kr

31   and Gabriel Núñez, Comprehensive Cancer Center, University of Michigan Medical

32   School, 1500 E. Medical Center Drive, Ann Arbor, MI 48109, USA.

33   E-mail: gabriel.nunez@umich.edu (Gabriel Núñez)

34

35   Short title: Microbiota enhances oral vaccination via Nod2 and IL-1β

36   This manuscript includes total 7 figures and 3 supplementary figures.**Summary**

37   The role of symbiotic bacteria in the development of antigen-specific immunity

38   remains poorly understood. Previous studies showed that sensing of symbiotic bacteria by

39   nucleotide-binding oligomerization domain containing protein 2 (Nod2) regulates antibody

40   responses in response to nasal immunization with antigen and cholera toxin (CT). In this

41   study, we examined the role of the microbiota in the adjuvant activity of CT induced after

42   oral immunization with antigen. Germ-free mice showed impaired production of antibody

43   responses and T cell-specific cytokines after oral immunization when compared to that

44   observed in conventionally raised mice. Similar to germ-free mice, Nod2-deficient mice

45   showed reduced humoral responses upon oral immunization with antigen and CT.

46   Treatment with CT enhanced the production of IL-1β, but not TNF-α or IL-12p40, induced

47 by stimulation of dendritic cells with muramyl dipeptide, the Nod2 ligand. Mechanistically,

48 the enhanced production of IL-1β induced by MDP and CT stimulation required Nod2 and

49 was mediated by both increased syntheses of pro-IL-1β and caspase-1 activation.

50 Furthermore, antigen-specific antibody and cytokine responses induced by CT were

51 impaired in orally immunized IL-1β-deficient mice. Collectively, our results indicate that

52 Nod2 stimulation by symbiotic bacteria contributes to optimal CT-mediated antigen-

53 specific oral vaccination through the induction of IL-1β production.

54

55 **Keywords:** Microbiota; Symbiotic bacteria; Cholera toxin; Adjuvant; Nod2; IL-1β

56 **Introduction**

57 Cholera toxin (CT), an enterotoxin secreted by the bacterium *Vibrio cholerae*, is

58 responsible for the massive diarrhea characteristic of cholera infection.[1] The CT protein

59 complex is composed of one A subunit and five B subunits. The A subunit exhibits ADP-

60 ribosyltransferase activity that activates the guanine-nucleotide binding protein Gsα and, in

61 turn, adenylate cyclase, thereby increasing intracellular levels of cyclic adenosine

62 monophosphate (cAMP). In contrast, the B subunit plays a role in the binding of the toxin

63 to GM1 ganglioside receptors found on the host cell surfaces.[1-4] CT is known to exhibit a

64 potent adjuvant activity, mainly linked to the activity of its monomeric A subunit.[5]

65 However, CT holotoxin is too toxic for human use.[1] Despite extensive studies on the

66 mechanism underlying the adjuvant activity of CT, the lack of sufficient understanding has

67 hampered the development of nontoxic, but effective adjuvants based on this toxin.

68 CT is known to promote mucosal and systemic immune responses. Treatment with

69 CT drives naïve T cells toward T_H2 type responses.[6, 7] However, other reports have shown

70 that the toxin also promotes T_H1 and T_H17 differentiation through a cAMP-dependent

71 pathway, which might be required for its adjuvant activity.[8, 9] CT activates T cells by

72 inducing the production of cytokines from antigen-presenting cells (APCs) and

73 costimulatory molecules on the cell surface.[10] In addition, the toxin enhances the antigen

74 presentation capacity of APCs, an initial step in the adaptive immune response, through a

75 cAMP-dependent pathway.[11, 12] Collectively these studies show that the effect of CT on

76 APCs might be critical to its ability to promote adaptive immunity.

77   The microbiota plays an important role in the induction of immune cell populations,

78 development of gut-associated lymphoid tissues and protection against viral and bacterial

79 infections.[13, 14] Moreover, the microbiota enhances immune responses induced by

80 unadjuvanted and inactivated influenza vaccines through stimulation of the Toll-like

81 receptor (TLR)5 receptor.[15] In addition, symbiotic bacteria located in the nasal cavity

82 enhance antibody responses induced by nasal immunization with antigen and CT.[16]

83 Although the gastrointestinal tract is where most symbiotic bacteria reside, the contribution

84 of the gut microbiota to oral vaccination remains unclear.

85   Members of the nucleotide-binding oligomerization domain (Nod)-like receptor

86 (NLR) family function as intracellular pattern recognition receptors (PRRs) to activate host

87 immunity in response to microbial products and damage-associated signals.[17] The NLR

88 family member Nod2 recognizes the muramyl dipeptide (MDP) motif which is conserved

89 in peptidoglycan produced by both Gram-negative and Gram-positive bacteria.[18-20] Upon

90 stimulation, Nod2 activates nuclear factor (NF)-κB and mitogen activated protein kinases

91 (MAPKs) to induce expression of pro-inflammatory and antimicrobial molecules.[18-21] MDP

92 exhibits adjuvant activity and induces predominant T_H2 responses and, in combination with

93 TLR agonists, promotes the production of a high level of antigen-specific antibody in

94 mice.[22, 23] In addition, Nod2-mediated recognition of the microbiota plays a critical role in

95 the mucosal adjuvant activity of CT induced via the nasal route.[16] Here, we examined the

96 role of the microbiota and Nod2 in antibody responses induced by oral immunization with

97 antigen and CT.

98 **Material and methods**

99 *Mice*

100   Wild-type (WT), *Nod2*$^{-/-}$, and *Ilb1*$^{-/-}$ mice on a C57BL/6 background were bred

101 and maintained under specific pathogen free (SPF) conditions at the University of Michigan

102 Animal Facility. C57BL/6 mice purchased from Orientbio Inc. (Seongnam, Korea) were

103   held under SPF conditions in an animal facility at Wide River Institute of Immunology of

104   Seoul National University College of Medicine. *Nod2*$^{-/-}$ mice were bred and held under

105   SPF conditions in an animal facility at Wide River Institute of Immunology of Seoul

106   National University College of Medicine. Germ-free (GF) C57BL/6 mice were bred and

107   maintained at the Germ-Free Animal Core Facility of the University of Michigan. Mice

108   were allocated randomly into experimental groups. We performed all experimental

109   procedures in accordance with protocols approved by the University Committee on Use and

110   Care of Animals at the University of Michigan and by the Institutional Animal Care and

111   Use Committee (IACUC) at the Seoul National University Hospital.

112

113   *Reagents*

114   CT (List Biological Laboratories), human serum albumin (HSA; Talecris

115   Biotherapeutics or Sigma), MDP (Bachem), Ultrapure LPS (InvivoGen), Pam3

116   (Pam3CSK4, InvivoGen), LTA (lipoteichoic acid, InvivoGen), PolyI:C (PolyI:C HMW,

117   InvivoGen), CpG (ODN 1826, InvivoGen), CT A subunit (List Biological Laboratories), 8-

118   Br-cAMP (Sigma), N6-benzoyl-cAMP (BioLog Life Science Institute), 8-CPT-2'-O-Me-

119   cAMP (Enzo life sciences), and H-89 (InvivoGen) were purchased from the indicated

120   commercial sources. IL-1β antibody was purchased from R&D Systems and antibodies for

121   glyceraldehyde 3-phosphate dehydrogenase (GAPDH) and β-actin were obtained from

122   Santa Cruz Biotechnology; antibody against caspase-1 was generated in our laboratory.

123

124   *Immunization protocol*

125   We orogastrically immunized 7–10-week-old age- and sex-matched mice with 200

126   μl of distilled water containing 10 mg of HSA and 10 μg of CT by gavage. Mice were

127   euthanized and then blood and spleen were obtained for analysis at 2 weeks after

128   immunization or at the indicated time points. For the GF experiments, all reagents were

129   autoclaved or passed through 0.2-μm filters (Corning) before immunization. No animals or

130   samples used in the mouse experiments were excluded from the analyses.

131

Measurement of HSA-specific antibodies

Mouse blood samples were collected in plasma separator tubes with lithium heparin (BD Biosciences) and plasma were separated by centrifugation. Mouse feces were suspended in PBS (100 mg/ml) by vigorous vortexing. ELISA plates were coated with HSA and the levels of HSA-specific total IgG, IgA, IgG_1, IgG_{2b}, and IgM were measured using a indirect ELISA method based on the manufacturer's instructions (SBA Clonotyping™ System/AP; SouthernBiotech).

139

Re-stimulation of splenocytes

Splenocytes were isolated from spleens on day 14 after immunization as previously described.[24] Briefly, spleens were mashed through a cell strainer (Falcon), and then the cells were spun down and resuspended in RBC lysis buffer (eBioscience). After 5 minutes, the cells were rinsed with complete RPMI medium containing 10% heat-inactivated fetal bovine serum, 2-β-mercaptoethanol (50 μM), L-glutamine (2 mM), sodium pyruvate (1 mM), MEM non-essential amino acids, and penicillin-streptomycin (Gibco) and pushed through the cell strainer. Isolated splenocytes (2×10^6 cells in 200 μl inoculated into each well in a 48-well plate) were resuspended in complete RPMI medium and re-stimulated with 500 μg/ml of HSA. After 4 days, culture supernatants were harvested and analyzed for cytokines by ELISA.

151

BMDC culture condition and in vitro stimulation

BMDCs (bone marrow derived dendritic cells) were generated by differentiating bone marrow progenitors isolated from femurs and tibiae of a mouse in RPMI medium containing 10% heat-inactivated FBS, 2-mercaptoethanol (50 μM), penicillin–streptomycin and 20 ng/ml of granulocyte–macrophage colony-stimulating factor (GM-CSF; PeproTech) and were supplemented with fresh medium on day 3 and day 5. On day 7 after bone

158   marrow isolation, non-adherent cells were collected as differentiated BMDCs by vigorous

159   aspiration. BMDCs (4×10^5 cells in 200 μl inoculated into each well in a 48-well plate)

160   were stimulated with MDP (10 μg/ml) or LPS (100 ng/ml), and, 30 minutes later, CT (500

161   ng/ml), CT A subunit (1 μg/ml), and cAMP derivatives (8-Br-cAMP (100 μM), 6-Bnz-

162   cAMP (50 μM), and 8-CPT-2'-O-Me-cAMP (50 μM)) were added. For selective inhibition

163   of the protein kinase A (PKA) signaling pathway, BMDCs were pretreated with H-89 (10

164   μM) before being treated with MDP for 30 minutes. Culture supernatants were harvested

165   for ELISA and immunoblotting and cells lysates were collected for immunoblotting and

166   real-time quantitative PCR (qPCR).

167

168   *Cytokines measurements*

169   Cytokines were measured using ELISA kits according to the manufacturer's

170   instructions (R&D Systems).

171

172   *Immunoblotting*

173   Cells were lysed in RIPA buffer supplemented with complete protease inhibitor

174   cocktail (Roche). Supernatants were mixed with loading buffer and then separated by SDS-

175   PAGE and transferred to PVDF membranes (Millipore). Membranes were incubated with

176   antibodies against all forms of IL-1β or caspase-1 (1:1000 dilution). Protein bands were

177   detected using an ECL kit (Thermo Scientific). Membranes were removed using restore

178   stripping buffer (Thermo Scientific) and re-probed with antibody against GAPDH (1:5000)

179   or β-actin (1:5000) as a loading control. The intensities of blots were measured by using

180   ImageJ program (NIH). Intensities of all samples were normalized by those of their loading

181   control and then the final numerical values were calculated as relative values against the

182   mean value of Nod2 deficient samples.

183

184   *Real-time qPCR*

185   RNA was extracted using an E.Z.N.A. Total RNA Kit I (Omega bio-tek) and cDNA

186   was then generated from the isolated RNA using a High capacity RNA-to-cDNA Kit

187   (Applied Biosystems). The cDNA was used for real-time qPCR with specific primer sets

188   and SYBR Green PCR Master Mix (Applied Biosystems) according to the manufacturer's

189   instruction for StepOnePlus Real-Time PCR systems (Applied Biosystems). The real-time

190   qPCR primers (Invitrogen) were as follows: IL-1β (5′-

191   CAACCAACAAGTGATATTCTCCATG-3′ and 5′-GATCCACACTCTCCAGCTGCA-3′)

192   and GAPDH (5′-TGCGACTTCAACAGCAACTC-3′ and 5′-

193   GCCTCTCTTGCTCAGTGTCC-3′). The real-time qPCR conditions for mRNA

194   quantification were 95 °C for 10 minutes, followed by 40 cycles of denaturation at 95 °C

195   for 15 seconds and annealing and extension at 60 °C for 1 minute. The cycle threshold (Ct)

196   values of respective samples were normalized internally using the average Ct value of

197   GAPDH.

198

199   *Statistical analyses*

200   Statistical analyses were performed using GraphPad Prism software (GraphPad

201   Software). For cytokine comparisons, linear regression with a 95% confidence interval, and

202   unpaired, two-tailed Student's *t*-test were used. We examined differences in the results

203   between groups of individual animals using the non-parametric Mann-Whitney test. No

204   samples or animals were excluded from the analyses. Differences with $p < 0.05$ were

205   considered statistically significant.

206   **Results**

207   **Symbiotic bacteria contribute to the efficacy of oral immunization with antigen and**

208   **cholera toxin**

209   We previously showed that antibiotic treatment reduces the efficacy of oral

210   immunization with the model antigen, HSA, and CT as an adjuvant.[16] Because treatment

211 with antibiotics does not completely deplete bacteria in the gastrointestinal tract,[25] we

212 compared immune responses between SPF and GF mice after oral immunization with HSA

213 and CT. Consistent with previous results following antibiotic treatment,[12, 16] the amounts of

214 HSA-specific immunoglobulin G (IgG) in the plasma of GF mice were reduced when

215 compared to those observed in conventionally raised SPF mice (Fig. 1a). In addition, when

216 mice were administrated with HSA or CT alone failed to produce HSA-specific IgG in SPF

217 mice (see Supplementary material, Fig. S1). These data confirm that commensal bacteria

218 play an important role in CT-mediated adjuvant effect on orally injected antigen. Moreover,

219 e*x vivo* re-stimulation of splenocytes derived from SPF mice with HSA showed increased

220 production of the T_H1 cytokine interferon (IFN)-γ, the T_H2 cytokine IL-5, and the T_H17

221 cytokine IL-17 in splenocytes, whereas the induction of T cell cytokines was significantly

222 suppressed in splenocytes from GF mice (Fig. 1b). These results indicate that symbiotic

223 bacteria play an important role in promoting the adjuvant activity of CT after oral

224 immunization.

225

226 **Nod2 receptor contributes to the adjuvant activity of cholera toxin**

227   To investigate the contribution of Nod2 to oral immunization with antigen and CT,

228 WT and *Nod2*$^{-/-}$ mice were orogastrically immunized with HSA and CT. The analysis

229 showed impaired antigen-specific antibody production in plasma from *Nod2*$^{-/-}$ mice when

230 compared with that in WT mice (Fig. 2a and see Supplementary material, Fig. S2). In

231 addition, the amounts of antigen-specific IgA in the feces of *Nod2*$^{-/-}$ mice were less than

232 that in the feces of WT mice (Fig. 2b). In line with these antibody responses, the production

233 of IL-5 and IL-17, induced by antigen re-stimulation, were lower in splenocytes from *Nod2*$^{-/-}$

234 *$^{/-}$* mice than in splenocytes from WT mice (Fig. 2c). The amount of IFN-γ produced after

235 antigen re-stimulation was also reduced in Nod2-deficient splenocytes when compared with

236 in WT splenocytes, although the difference was not statistically significant (Fig. 2c). These

237 data suggest that Nod2 recognition of the symbiotic bacteria is important for the adjuvant

238 activity induced by oral immunization with CT.

239

Nod2 ligand and cholera toxin act synergistically to enhance IL-1β production in DCs

Because Nod2 in CD11c^{+} cells plays an important role in the adjuvant activity of CT administered via the nasal route,[16] we examined the regulation of cytokine production by the Nod2 ligand MDP and CT in *in vitro* experiments using bone marrow derived dendritic cells (DCs). To mimic conditions in the intestinal tract after oral immunization, we pretreated DCs cells with microbe-associated molecular patterns (MAMPs) for 30 min and then stimulated the cells with CT. Sequential treatment with MDP and CT led to a synergetic induction of IL-1β secretion, but not of TNF-α (Fig. 3a). Unlike IL-1β which was not induced by treatment of MDP alone, IL12p40 was induced by single treatment with both MDP and CT. Increased secretion of IL12p40 from cells sequentially treated with MDP and CT can be ascribed to cumulative stimulation by MDP and CT, rather than synergistic enhancement (Fig. 3a). In contrast to MDP, the ability of multiple TLR agonists including those for TLR1/2, TLR2/6, TLR3, TLR4, and TLR9 to stimulate the production of IL-1β was minimally or no enhanced by CT (see Supplementary material, Fig. S3a and S3b). To examine the kinetics and Nod2 dependence of IL-1β production by MDP and CT stimulation, we pretreated DCs from WT and *Nod2^{-/-}* mice with MDP or medium and then treated the cells with CT or control. Treatment with MDP and CT induced IL-1β production in a synergic manner compared to treatment with MDP or CT alone in WT DCs (Fig. 3b). In contrast, the enhancement of IL-1β production by MDP and CT was not observed in DCs from *Nod2^{-/-}* mice (Fig. 3b).

260

CT enhances IL-1β production by increasing pro-IL-1β expression and caspase-1 activation

To understand the mechanism by which CT enhances the secretion of IL-1β in MDP-stimulated DCs, we first assessed the production of pro-IL-1β in DCs pre-stimulated with MDP or LPS followed by treatment with CT by immunoblotting. In the absence CT stimulation, there was little or no induction of pro-IL-1β by MDP while LPS induced pro-

267   IL-1β (Fig. 4a). In contrast, CT treatment induced robust production of pro-IL-1β in DCs

268   pretreated with MDP compared with DCs treated with CT alone (Fig. 4a). Importantly, the

269   enhancement of pro-IL-1β production in MDP-stimulated DCs by CT was not observed in

270   the absence of Nod2 (Fig. 4a), indicating that the synergism between MDP and CT requires

271   the expression of Nod2 in DCs. In contrast to MDP, treatment with CT did not enhance the

272   production of pro-IL-1β induced by LPS (Fig. 4a), consistent with previous results (Fig.

273   S2). To determine whether CT enhances the expression of *Il1b* mRNA, we pretreated DCs

274   from WT and *Nod2*^{-/-} mice with MDP or medium and then treated the cells with CT or not.

275   Sequential treatment with MDP and CT induced *Il1b* mRNA in a synergic manner

276   compared to treatment with MDP or CT alone in WT DCs (Fig. 4b) which parallels that

277   observed with IL-1β protein release (Fig. 3b). As expected, the enhancement of *Il1b* mRNA

278   production by MDP and CT was not observed in DCs from *Nod2*^{-/-} mice (Fig. 4b).

279   The secretion of mature IL-1β is regulated via two-step process that includes the

280   induction of pro-IL-1β and the proteolytic activation of caspase-1 that cleaves pro-IL-1β.[26]

281   To determine whether MDP and CT also regulate the activation of caspase-1, we assessed

282   the processing of caspase-1 and production of pro-IL-1β in DCs in the presence and

283   absence of MDP and/or CT stimulation by immunoblotting. Consistent with results shown

284   in Fig. 4a, CT enhanced the production of pro-IL-1β in DCs pre-stimulated with MDP (Fig.

285   4c). Importantly, treatment with CT induced the proteolytic activation of caspase-1 in

286   untreated and MDP-treated DCs (Fig. 4c). These results indicate that CT regulates the

287   release of IL-1β by enhancing both the production of pro-IL-1β and inducing the activation

288   of caspase-1 in MDP-stimulated DCs.

289

290   **CT enhances the production of IL-1β via cAMP/PKA signaling**

291   CT stimulates adenylate cyclase to increase the intracellular cAMP concentration

292   which has been linked to its adjuvant activity.[1, 4] Elevated intracellular cAMP in turn PKA

293   or Rap guanine nucleotide exchange factors (also known as exchange protein directly

294   activated by cAMP (Epac) 1 and 2), which regulate specific cellular functions.[9, 27] To

295   determine whether cAMP, PKA, and/or Epac are involved in MDP and CT-mediated IL-1β

296   induction, we treated DCs with cell permeable cAMP analog (8-bromo-cAMP), PKA

297   activator (N^6-benzoyl-cAMP), or Epac activator (8-CPT-2′-O-Me-cAMP) after

298   pretreatment with MDP. Like CT, treatment with 8-bromo-cAMP or N^6-benzoyl-cAMP

299   enhanced the ability of MDP to induce the secretion of IL-1β (Fig. 5a). In contrast,

300   treatment with 8-CPT-2′-O-Me-cAMP did not enhance the secretion of IL-1β (Fig. 5b).

301   These results suggest that CT enhances pro-IL-1β production via cAMP and PKA, but not

302   Epac activation. Consistent with these observations, treatment with 8-bromo-cAMP or N^6-

303   benzoyl-cAMP, but not 8-CPT-2′-O-Me-cAMP, enhanced the ability of MDP to induce the

304   production of pro-IL-1β (Fig. 5b). To confirm the role of the PKA signaling pathway in IL-

305   1β induction by MDP and CT, DCs were treated with a selective inhibitor of PKA, H-89,

306   before sequential stimulation with MDP and CT. Consistent with results obtained with the

307   use of an activator of PKA, the ability of CT to synergize with MDP in the production of

308   IL-1β in DCs was suppressed by pretreatment with H-89 (Fig. 5c). Collectively, these

309   results indicate that CT enhances the production of IL-1β in MDP-stimulated DCs via

310   cAMP/PKA signaling.

311

312   **Nod2 is required for IL-1β induction after oral immunization with antigen and**

313   **cholera toxin.**

314   To determine whether the production of IL-1β is induced in response to oral

315   immunization *in vivo*, we orogastrically immunized mice with HSA and CT, and then the

316   spleens were isolated at the indicated time point to examine the levels of *Il1b* mRNA. The

317   amounts of *Il1b* mRNA in the spleens increased by 3 days following oral immunization and

318   declined to basal levels by 9 days following oral immunization (Fig. 6a). To examine

319   whether Nod2 is involved in the induction of IL-1β, the expression of pro-IL-1β was

320   examined in the spleens from WT and *Nod2$^{-/-}$* mice on day 3 after oral immunization with

321   antigen and CT. As shown in Fig. 6b, pro-IL-1β expression was markedly reduced in the

322   spleen of *Nod2$^{-/-}$* mice compared to that of control WT mice. Likewise, when we

323   investigated Peyer's patches (PPs) isolated from ileum on day 1 after oral immunization,

324 deficiency of Nod2 reduced the pro-IL-1β expression as compared to that of control PPs

325 (Fig. 6c). These results suggest that oral immunization with antigen and CT increases IL-1β

326 expression in the spleen and PPs via Nod2.

327

328 **IL-1β is important for the adjuvant activity of cholera toxin.**

329   To determine whether the role of IL-1β in the adjuvant activity of CT, we

330 orogastrically immunized WT and $Il1b^{-/-}$ mice with HSA and CT. Similar to that observed

331 in $Nod2^{-/-}$ mice, the production of antigen-specific IgG was impaired in $Il1b^{-/-}$ mice

332 compared to that detected in WT mice (Fig. 7a). Moreover, the production of T cell

333 cytokines, IFN-γ, IL-5, and IL-17, which was increased by ex $vivo$ antigen re-stimulation

334 was markedly reduced in splenocytes from IL-1β-deficient mice when compared to

335 splenocytes from WT mice (Fig. 7b). These results indicate that IL-1β plays an important

336 role in the adjuvant activity of CT administered orally. **Discussion**

337   The efficacy of mucosal vaccines differs in various geographical regions.[28, 29] There

338 have been several hypotheses to explain the variation in immune responses after mucosal

339 vaccination. For example, malnutrition may contribute to oral vaccination in developing

340 countries.[30] In addition, an unsanitary environment in developing countries could lead to

341 persistent exposure of people to various enteric pathogens, which may be associated with

342 reduced efficacy of mucosal vaccines.[31] A major finding of this study is that the microbiota

343 plays a crucial role in oral immunization with antigen and CT. Thus, our results raise the

344 possibility that differences in the composition of the microbiota among individuals may

345 affect the efficacy of oral vaccination. The composition of the gut microbiota varies widely

346 among individuals and can be affected by various environmental factors, including dietary

347 habits, pathogen infections and geographical location.[32] Thus, well-designed

348 epidemiological studies are needed to examine the effects of the microbiota on vaccination

349 efficacy and if the microbiota plays a role, it will be important to design appropriate

350 vaccine protocols to overcome any limitations to elicit protective immune responses due to

351 specific microbiota profile.

352   Successful vaccination is the result of orchestrated innate and adaptive immune

353   responses.[33] Given that innate immune signals modulate the magnitude, quality, and

354   duration of adaptive responses,[33] many MAMPs, which promote innate immune signals

355   through host PRRs,[34] have been studied as adjuvant candidates and, among them, a TLR

356   ligand adjuvant has been approved for the clinical use with a human papillomavirus

357   vaccine.[33, 35] MDP, a Nod2 ligand, was originally identified as the active component in the

358   adjuvanticity of complete Freund's adjuvant (CFA) and several studies have reported its

359   potential for use as a non-mucosal adjuvant.[22, 36] We recently showed that, upon

360   immunization via the nasal route, MDP enhanced the adjuvant activity of CT, even though

361   MDP itself has no mucosal adjuvant activity.[16] Likewise, the significance of the Nod2

362   receptor in the adjuvant activity of CT via the oral route was confirmed in this study, which

363   suggests that MDP delivered in concert with CT may exhibit potent mucosal adjuvant

364   activity. Thus, the development of less pyrogenic and more potent adjuvants based on

365   derivatives of CT and MDP should be considered. For example, like CTA1-DD, a fusion

366   protein of CT A subunit and the cell-binding domain of *Staphylococcus aureus*,[37] a

367   molecule that combines the CT A subunit and MDP derivatives might be effective in

368   providing enhanced adjuvant activity.

369   DCs and macrophages are important mediators of the adjuvant activity of CT.[38, 39]

370   Consistently, expression of Nod2 receptor in CD11c$^+$ cells, including DCs, is required for

371   optimal elicitation of an adaptive immune response by nasal immunization with antigen and

372   CT.[16] In the current work, we show that Nod2 is also important for the induction of

373   antibody responses in response to oral immunization with antigen and CT. Furthermore, we

374   found that IL-1β is a critical mediator of the adjuvant activity of CT induced via the oral

375   route. Mechanistically, the production of IL-1β was induced synergistically by stimulation

376   of DCs with the Nod2 agonist and CT via induction of pro-IL-1β and caspase-1 activation.

377   These observations suggest that CT induces its adjuvant activity, at least part, by enhancing

378   the Nod2-stimulatory activity of the microbiota to induce IL-1β in intestinal DCs. IL-1β is a

379   pleiotropic cytokine that has a pivotal role in the onset and development of immune

380   responses.[40] In line with our observations, administration of recombinant IL-1β induces

381 adjuvant activity in both mucosal and systemic immunization protocols.[41-43] Even

382 recombinant *Lactobacillus casei*, which was engineered to produce biologically active IL-

383 1β, can function as an adjuvant in oral immunization.[44] However, the use of IL-1β as an

384 adjuvant has never been pursued because of its overwhelming inflammatory effects.[42] CT

385 induced IL-1β production at least in part by enhancing the expression of pro-IL-1β in

386 MDP-stimulated DCs via a cAMP-PKA dependent pathway. Many other adjuvants

387 originating from bacterial toxins, such as heat-labile toxin from *Escherichia coli* and

388 pertussis toxin and adenylate cyclase toxin from *Bordetella pertussis*, either directly or

389 indirectly increase the concentration of intracellular cAMP.[5, 45-47] Although correlation

390 between the increased cAMP and their adjuvanticity is controversial,[46, 47] our observations

391 with CT suggest that Nod2 ligand or bacteria having high Nod2 activity could also improve

392 the adjuvant activity of others toxins through induction of IL-1β production.

Acknowledgements

406

Disclosures

408 The authors have no conflicting interests to declare.

409

References

1   Holmgren J. Actions of cholera toxin and the prevention and treatment of cholera. *Nature* 1981; **292**:413-7.

2   Holmgren J, Lonnroth I and Svennerholm L. Tissue receptor for cholera exotoxin: postulated structure from studies with GM1 ganglioside and related glycolipids. *Infect Immun* 1973; **8**:208-14.

3   Katada T and Ui M. Direct modification of the membrane adenylate cyclase system by islet-activating protein due to ADP-ribosylation of a membrane protein. *Proc Natl Acad Sci USA* 1982; **79**:3129-33.

4   Cassel D and Pfeuffer T. Mechanism of cholera toxin action: covalent modification of the guanyl nucleotide-binding protein of the adenylate cyclase system. *Proc Natl Acad Sci USA* 1978; **75**:2669-73.

5   Lycke N, Tsuji T and Holmgren J. The adjuvant effect of *Vibrio cholerae* and *Escherichia coli* heat-labile enterotoxins is linked to their ADP-ribosyltransferase activity. *Eur J Immunol* 1992; **22**:2277-81.

6   Xu-Amano J, Kiyono H, Jackson RJ, Staats HF, Fujihashi K, Burrows PD, et al. Helper T cell subsets for immunoglobulin A responses: oral immunization with tetanus toxoid and cholera toxin as adjuvant selectively induces Th2 cells in mucosa associated tissues. *J Exp Med* 1993; **178**:1309-20.

7   Yamamoto S, Kiyono H, Yamamoto M, Imaoka K, Yamamoto M, Fujihashi K, et al. A nontoxic mutant of cholera toxin elicits Th2-type responses for enhanced mucosal immunity. *Proc Natl Acad Sci USA* 1997; **94**:5267-72.

8   Datta SK, Sabet M, Nguyen KPL, Valdez PA, Gonzalez-Navajas JM, Islam S, et al. Mucosal adjuvant activity of cholera toxin requires Th17 cells and protects against inhalation anthrax. *Proc Natl Acad Sci USA* 2010; **107**:10638-43.

9   Li X, Murray F, Koide N, Goldstone J, Dann SM, Chen J, et al. Divergent requirement for Gαs and cAMP in the differentiation and inflammatory profile of distinct mouse Th subsets. *J Clin Invest* 2012; **122**:963-73.

10   Martin M, Metzger DJ, Michalek SM, Connell TD and Russell MW. Distinct Cytokine Regulation by Cholera Toxin and Type II Heat-Labile Toxins Involves Differential Regulation of CD40 Ligand on CD4(+) T Cells. *Infect Immun* 2001; **69**:4486-92.

11   Kawamura YI, Kawashima R, Shirai Y, Kato R, Hamabata T, Yamamoto M, et al. Cholera toxin activates dendritic cells through dependence on GM1-ganglioside which is mediated by NF-κB translocation. *Eur J Immunol* 2003; **33**:3205-12.

12   Bromander A, Holmgren J and Lycke N. Cholera toxin stimulates IL-1 production and enhances antigen presentation by macrophages *in vitro*. *J Immunol* 1991; **146**:2908-14.

13   Kamada N, Seo S-U, Chen GY and Nunez G. Role of the gut microbiota in immunity and inflammatory disease. *Nat Rev Immunol* 2013; **13**:321-35.

443   14   Kim D, Zeng MY and Núñez G. The interplay between host immune cells and gut microbiota in chronic
444   inflammatory diseases. *Exp Mol Med* 2017; **49**:e339.

445   15   Oh Jason Z, Ravindran R, Chassaing B, Carvalho Frederic A, Maddur Mohan S, Bower M, et al. TLR5-
446   Mediated Sensing of Gut Microbiota Is Necessary for Antibody Responses to Seasonal Influenza
447   Vaccination. *Immunity* 2014; **41**:478-92.

448   16   Kim D, Kim Y-G, Seo S-U, Kim D-J, Kamada N, Prescott D, et al. Nod2-mediated recognition of the
449   microbiota is critical for mucosal adjuvant activity of cholera toxin. *Nat Med* 2016; **22**:524-30.

450   17   Shaw MH, Reimer T, Kim Y-G and Nuñez G. NOD-like receptors (NLRs): bona fide intracellular
451   microbial sensors. *Curr Opin Immunol* 2008; **20**:377-82.

452   18   Inohara N, Ogura Y, Fontalba A, Gutierrez O, Pons F, Crespo J, et al. Host Recognition of Bacterial
453   Muramyl Dipeptide Mediated through NOD2: IMPLICATIONS FOR CROHN′S DISEASE. *J Biol*
454   *Chem* 2003; **278**:5509-12.

455   19   Girardin SE, Boneca IG, Viala J, Chamaillard M, Labigne A, Thomas G, et al. Nod2 Is a General Sensor
456   of Peptidoglycan through Muramyl Dipeptide (MDP) Detection. *J Biol Chem* 2003; **278**:8869-72.

457   20   Park J-H, Kim Y-G, McDonald C, Kanneganti T-D, Hasegawa M, Body-Malapel M, Inohara N and
458   Núñez G. RICK/RIP2 Mediates Innate Immune Responses Induced through Nod1 and Nod2 but Not
459   TLRs. *J Immunol*. 2007; **178**:2380-6.

460   21   Hasegawa M, Fujimoto Y, Lucas PC, Nakano H, Fukase K, Núñez G, et al. A critical role of RICK/RIP2
461   polyubiquitination in Nod-induced NF-κB activation. *EMBO J* 2008; **27**:373-83.

462   22   Magalhaes JG, Fritz JH, Le Bourhis L, Sellge G, Travassos LH, Selvanantham T, et al. Nod2-Dependent
463   Th2 Polarization of Antigen-Specific Immunity. *J Immunol* 2008; **181**:7925-35.

464   23   Pavot V, Rochereau N, Rességuier J, Gutjahr A, Genin C, Tiraby G, et al. Cutting Edge: New Chimeric
465   NOD2/TLR2 Adjuvant Drastically Increases Vaccine Immunogenicity. *J Immunol* 2014; **193**:5781-5.

466   24   Kim D, Kim SH, Park E-J, Kim J, Cho S-H, Kagawa J, et al. Suppression of allergic diarrhea in murine
467   ovalbumin-induced allergic diarrhea model by PG102, a water-soluble extract prepared from *Actinidia*
468   *arguta*. *Int Arch Allergy Immunol* 2009; **150**:164-71.

469   25   Ubeda C, Taur Y, Jenq RR, Equinda MJ, Son T, Samstein M, et al. Vancomycin-resistant Enterococcus
470   domination of intestinal microbiota is enabled by antibiotic treatment in mice and precedes bloodstream
471   invasion in humans. *J Clin Invest* 2010; **120**:4332-41.

472   26   He Y, Hara H and Núñez G. Mechanism and Regulation of NLRP3 Inflammasome Activation. *Trends*
473   *Biochem Sci* 2016; **41**:1012-21.

474   27   de Rooij J, Zwartkruis FJ, Verheijen MH, Cool RH, Nijman SM, Wittinghofer A, et al. Epac is a Rap1
475   guanine-nucleotide-exchange factor directly activated by cyclic AMP. *Nature* 1998; **396**:474-7.

476   28   Steele AD, Patel M, Parashar UD, Victor JC, Aguado T and Neuzil KM. Rotavirus Vaccines for Infants
477   in Developing Countries in Africa and Asia: Considerations from a World Health Organization–
478   Sponsored Consultation. *J Infect Dis* 2009;**200**:S63-9.

479 29 Levine MM. Immunogenicity and efficacy of oral vaccines in developing countries: lessons from a live
480   cholera vaccine. *BMC Biol* 2010; **8**:129.

481 30 Prendergast AJ. Malnutrition and vaccination in developing countries. *Philos Trans R Soc Lond B Biol*
482   *Sci* 2015; **370**:20140141.

483 31 Korpe PS and Petri WA. Environmental Enteropathy: Critical implications of a poorly understood
484   condition. *Trends Mol Med* 2012; **18**:328-36.

485 32 Cordain L, Eaton SB, Sebastian A, Mann N, Lindeberg S, Watkins BA, et al. Origins and evolution of
486   the Western diet: health implications for the 21st century. *Am J Clin Nutr* 2005; **81**:341-54.

487 33 Freytag LC and Clements JD. Mucosal adjuvants. *Vaccine* 2005; **23**:1804-13.

488 34 Palm NW and Medzhitov R. Pattern recognition receptors and control of adaptive immunity. *Immunol*
489   *Rev* 2009; **227**:221-33.

490 35 Schwarz T. Clinical update of the AS04-Adjuvanted human Papillomavirus-16/18 cervical cancer
491   vaccine, cervarix®. *Adv Ther* 2009; **26**:983-98.

492 36 Ellouz F, Adam A, Ciorbaru R and Lederer E. Minimal structural requirements for adjuvant activity of
493   bacterial peptidoglycan derivatives. *Biochem Biophys Res Commun* 1974; **59**:1317-25.

494 37 Mowat AMI, Donachie AM, Jägewall S, Schön K, Löwenadler B, Dalsgaard K, et al. CTA1-DD-
495   Immune Stimulating Complexes: a Novel, Rationally Designed Combined Mucosal Vaccine Adjuvant
496   Effective with Nanogram Doses of Antigen. *J Immunol* 2001; **167**:3398-405.

497 38 Gagliardi MC, Sallusto F, Marinaro M, Langenkamp A, Lanzavecchia A, and De Magistris MT. Cholera
498   toxin induces maturation of human dendritic cells and licences them for Th2 priming. *Eur J Immunol*
499   2000; **30**:2394-403.

500 39 Yamamoto M, Kiyono H, Yamamoto S, Batanero E, Kweon MN, Otake S, et al. Direct effects on
501   antigen-presenting cells and T lymphocytes explain the adjuvanticity of a nontoxic cholera toxin mutant.
502   *J Immunol* 1999; **162**:7015-21.

503 40 Dinarello CA. Biologic basis for interleukin-1 in disease. *Blood* 1996; **87**:2095-147.

504 41 Staats HF and Ennis FA. IL-1 Is an Effective Adjuvant for Mucosal and Systemic Immune Responses
505   When Coadministered with Protein Immunogens. *J Immunol* 1999; **162**:6141-7.

506 44 Kusnecov AW and Rossi-George A. Potentiation of Interleukin-1β Adjuvant Effects on the Humoral
507   Immune Response to Antigen in Adrenalectomized Mice. *Neuroimmunomodulation* 2001; **9**:109-18.

508 43 Rothel JS, Seow HF, Lightowlers MW, Parry BW, Gauci C, Hurst L, et al. The use of recombinant
509   ovine IL-1β and TNF-α as natural adjuvants and their physiological effects *in vivo*. *Immunol Cell Biol*
510   1998; **76**:167-72.

511 44 Kajikawa A, Masuda K, Katoh M and Igimi S. Adjuvant Effects for Oral Immunization Provided by
512   Recombinant *Lactobacillus casei* Secreting Biologically Active Murine Interleukin-1β. *Clin Vaccine*
513   *Immunol* 2010; **17**:43-8.

514   45   Johnson AM, Kaushik RS, Francis DH, Fleckenstein JM and Hardwidge PR. Heat-Labile Enterotoxin

515   Promotes *Escherichia coli* Adherence to Intestinal Epithelial Cells. *J Bacteriol* 2009; **191**:178-86.

516   46   Liang S, Hajishengallis G. Heat-labile enterotoxins as adjuvants or anti-inflammatory agents. *Immunol*

517   *Invest* 2002; **39**:449-67.

518   47   Bagley KC, Abdelwahab SF, Tuskan RG, Fouts TR and Lewis GK. Pertussis toxin and the adenylate

519   cyclase toxin from *Bordetella pertussis* activate human monocyte-derived dendritic cells and dominantly

520   inhibit cytokine production through a cAMP-dependent pathway. *J Leukoc Biol* 2002; **72**:962-9.

521

522

523

Supporting Information

525   Additional Supporting Information may be found in the online version of this article.

526   **Figure. S1.** Production of antigen-specific IgG is induced by oral immunization with both

527   HSA and cholera toxin, but not CT or HSA alone or mock control. The relative amount of

528   HSA-specific IgG was determined in plasma of SPF mice on day 14 after oral

529   immunization with or without HSA and/or CT. Data are shown as means ± SEM. **p <

530   0.01 by Mann-Whitney test.

531   **Figure. S2.** Productions of antigen-specific IgG_1, IgG_{2b}, and IgM induced by oral

532   immunization with HSA and cholera toxin are suppressed in Nod2-deficient mice. The

533   relative amounts of HSA-specific IgG_1, IgG_{2b}, and IgM were determined in plasma of WT

534   ($n = 5$) and $Nod2^{-/-}$ ($n = 4$) mice on day 14 after oral immunization with HSA and CT. The

535   results are representative of two independent experiments. Data are shown as means ± SEM.

536   *p < 0.05 by Mann-Whitney test.

537   **Figure. S3.** Nod1 or TLR agonists have no synergetic effect with cholera toxin on IL-1β

538   production in dendritic cells. BMDCs were first treated with Pam3 (1 μg/ml), LTA (10

539   μg/ml), PolyI:C (50 μg/ml), LPS (0.1 μg/ml), and CpG (10 μg/ml) or left untreated (a), and

540   indicated concentration of Pam3, LPS, CpG (b). After 30 minutes, the cells were either

541 stimulated with CT (0.5 μg/ml) or left unstimulated for 24 hours. IL-1β in triplicate

542 supernatant samples was measured using ELISA. Data are shown as means ± SD.

543

544

Figure legends

546 **Figure. 1.** Symbiotic bacteria are critical for the oral adjuvant activity of cholera toxin. (a)

547 The levels of HSA-specific IgG were analyzed in plasma obtained from GF ($n = 7$) and

548 conventionally raised (specific pathogen-free; SPF) ($n = 5$) mice on day 14 post oral

549 immunization with 10 mg of HSA and 10 μg of CT. The left panel shows the relative

550 amounts of antigen-specific IgG in the serially diluted plasma as means ± SEM of the

551 optical density at 405 nm (OD405nm). The right panel displays HSA-specific IgG in the

552 plasma diluted 62.5 fold. Each dot in the right panel represents an individual mouse and the

553 means are displayed as a line. (b) Splenocytes isolated from immunized GF and SPF mice

554 on day 14 post immunization were re-stimulated with 500 μg/ml of HSA. IL-5, IL-17, and

555 IFN-γ were measured in triplicate supernatant samples on day 4 after stimulation; values

556 represent means ± SD. The results are representative of two independent experiments. *$p <$

557 0.05, **$p < 0.01$, and ***$p < 0.001$ by Mann-Whitney test (a) and two-tailed t-test (b). ND,

558 not detected.

559

560 **Figure. 2.** Nod2 plays a crucial role in promoting the adjuvant activity of cholera toxin. (a,

561 b) WT ($n = 5$ or 7) and *Nod2$^{-/-}$* ($n = 4$) mice were orogastrically immunized with 10 mg of

562 HSA and 10 μg of CT, and plasma and feces were collected on day 14 post oral

563 immunization. The relative amounts of antigen-specific IgG (a) and IgA (b) were measured

564 in serially diluted plasma and feces (100 mg/ml in PBS), respectively, and the results are

565 displayed in the left panels. Right panels show HSA-specific IgG (a) and IgA (b) in the

566 plasma diluted 62.5 fold and 5 fold, respectively. Each dot in the right panels represents an

567 individual mouse, and the means are displayed as a line. (c) Splenocytes were isolated from

568 WT and *Nod2$^{-/-}$* mice on day 14 post immunization and then re-stimulated with or without

569   HSA for 4 days. The amounts of IL-5, IL-17, and IFN-γ in triplicate supernatant samples

570   were measured by ELISA. The results are representative of two (b) or three (a, c)

571   independent experiments. Data are shown as means ± SEM (a, b) or ± SD (c). *$p < 0.05$,

572   **$p < 0.01$, and ***$p < 0.001$ by Mann-Whitney test (a, b) and by two-tailed t-test (c). ND,

573   not detected. NS, not significant.

574

575   **Figure. 3.** Nod2 ligand and cholera toxin act synergistically to enhance IL-1β production in

576   DCs. (a, b) BMDCs from WT (a, b) and $Nod2^{-/-}$ (b) mice were first treated with MDP (10

577   μg/ml) or left untreated, and, 30 minutes later, the cells were either stimulated with CT (0.5

578   μg/ml) or left unstimulated. The supernatants were collected at 24 hours (a) or at the

579   indicated time points (b) after CT addition. The indicated cytokines in triplicate supernatant

580   samples were measured by ELISA. Results are representative of two (b) or three (a)

581   independent experiments. Data are shown as means ± SD. *$p < 0.05$, **$p < 0.01$, and ***p

582   < 0.001 by two-tailed t-test for comparisons between all samples (a) and between sequential

583   treatment with MDP and CT and treatment with CT alone (b). ND, not detected.

584

585   **Figure. 4.** CT enhances IL-1β production by increasing pro-IL-1β expression and caspase-1

586   activation. (a–c). BMDCs from WT (a-c) and $Nod2^{-/-}$ (a, b) mice were treated with MDP

587   (10 μg/ml), LPS (100 ng/ml) or left untreated, and, 30 minutes later, the cells were either

588   stimulated with CT (0.5 μg/ml) or left unstimulated. Samples were collected at 18 hours (a)

589   or at the indicated time points (b, c) after CT addition. (a, c) Pro-IL-1β and GAPDH were

590   detected in cell lysates and pro-caspase-1 and p20 (the active form of caspase-1) were

591   analyzed in supernatants by immunoblotting. GAPDH was used as a loading control. (b)

592   The amount of $Il1b$ mRNA was determined by real-time qPCR and normalized relative to

593    $Gapdh$ expression. Data are shown as means ± SD. Results are representative of two

594   independent experiments.

595

596　**Figure. 5.** CT enhances the production of IL-1β in MDP-stimulated DCs via cAMP/PKA

597　signaling. (a–c) BMDCs were treated with MDP (10 μg/ml) or left untreated, and, 30

598　minutes later, the cells were either stimulated with CT (0.5 μg/ml), CT A subunit (CTA; 1

599　μg/ml), 8-Br-cAMP (cAMP; 100 μM), 6-Bnz-cAMP (Bnz; 50 μM), 8-CPT-2'-O-Me-cAMP

600　(CPT; 50 μM) or left unstimulated. (c) BMDCs were pretreated with the PKA inhibitor H-

601　89 (10 μM) at 30 minutes before sequential addition of MDP and CT. Cell lysates and

602　supernatants were collected at 18 hours (b) or 24 hours (a, c) after CT addition, respectively.

603　(a, c) IL-1β in triplicate supernatant samples was measured by ELISA. (b) Pro-IL-1β and

604　GAPDH were detected in cell lysates by immunoblotting. GAPDH was used as a loading

605　control. (a, c) Data are shown as means ± SD. ND, not detected. $*p < 0.05$, $**p < 0.01$, and

606　$***p < 0.001$ by two-tailed t-test for comparisons between sequential treatment with MDP

607　and CT and treatment with CT alone or between sequential treatments with MDP and CT.

608

609　**Figure. 6.** IL-1β expression induced by oral immunization with antigen and cholera toxin

610　depends on *Nod2*. (a, b, c) WT (n = 5, 3, or 2) (b, c) and *Nod2*$^{-/-}$ (n = 3 or 2) mice were

611　orogastrically immunized with HSA and CT, and spleens were collected at the indicated

612　time points (a) and on day 3 (b) post oral immunization. (c) Peyer's patches were isolated

613　from ileum on day 1 post oral immunization. (a) *Il1b* mRNA expression was analyzed by

614　real-time qPCR. *Gapdh* expression was used to normalize data. (b, c) Pro-IL-1β protein was

615　detected by immunoblotting, with β-actin as an internal control. Each lane represents an

616　individual mouse. The relative intensities of pro-IL-1β blots indicated below each lane were

617　normalized by their β-actin amounts and then were displayed as relative values against the

618　mean value of Nod2 deficient samples. The results are representative of two independent

619　experiments.

620

621　**Figure. 7.** IL-1β plays a crucial role in promoting the adjuvant activity of cholera toxin. (a)

622　The relative amounts of HSA-specific IgG were measured in the plasma of WT (n = 6) and

623　*Il1b*$^{-/-}$ (n = 5) mice on day 14 after oral immunization with HSA and CT. The left panel

624   shows the relative amounts of antigen-specific IgG in the serially diluted plasma as means

625   ± SEM. The right panel displays antigen-specific IgG in the plasma diluted 62.5 fold. Each

626   dot in the right panel represents an individual mouse, and the means are displayed as a line.

627   (b) Splenocytes were isolated from WT and *Il1b*$^{-/-}$ mice on day 14 post immunization and

628   then re-stimulated with HSA or left unstimulated for 4 days. IL-5, IL-17, and IFN-γ in

629   triplicate supernatant samples were measured by ELISA. Data are shown as means ± SD.

630   The results are representative of three independent experiments. *$p < 0.05$, **$p < 0.01$, and

631   ***$p < 0.001$ by Mann-Whitney test (a) and by two-tailed *t*-test (b). ND, not detected.
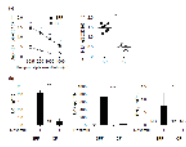
Figure 1. Kim et al.

imm_13105_f1.tif
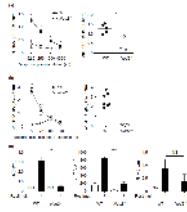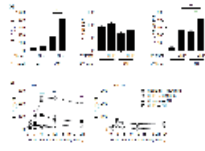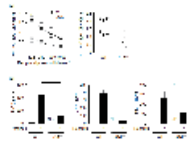
Figure 2. Kim et al.

imm_13105_f2.tif

imm_13105_f3.tif
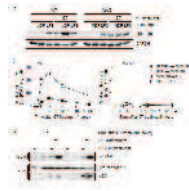
Figure 4 Kim et al.
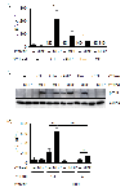
imm_13105_f4.tif

Figure 6. Kim et al.

imm_13105_f5.tif

imm_13105_f7.tif